Biosensors and Bioelectronics 87 (2017) 794–801

Contents lists available at ScienceDirect

Biosensors and Bioelectronics

journal homepage: www.elsevier.com/locate/bios

An electrochemical lipopolysaccharide sensor based on an immobilized Toll-Like Receptor-4

R.M. Mayall[a], M. Renaud-Young[a], N.W.C. Chan[b], V.I. Birss[a,*]

[a] Department of Chemistry, University of Calgary, 2500 University Drive NW, Calgary, AB, Canada T2N 1N4
[b] Defence Research and Development Canada, Suffield Research Centre, PO Box 4000, Station Main, Medicine Hat, AB, Canada T1A 8K6

ARTICLE INFO

Keywords:
Toll-Like Receptor-4
Electrochemical biosensor
Self-assembled monolayer
Impedance spectroscopy
Lipopolysaccharide
Gram-negative bacteria

ABSTRACT

Infections affect millions of people each year and yet methods to ascertain their cause can take more than 24 h to be effective. This delay between the presentation with symptoms and the ability to make an informed decision about treatment can have adverse consequences, including death in severe cases. Additionally, pathogen identification is a concern for public safety amid the growing threat of bioterrorism. Developing a detection system based on the immune system offers the advantage of broad specificity, while still remaining pertinent to human health. In this work, human Toll-Like Receptor-4 (TLR-4), a protein responsible for detecting lipopolysaccharide (LPS) of Gram-negative bacteria, was immobilized on both a large area and micro gold electrode via the tethering interaction of a modified Self-Assembled Monolayer (mSAM). In response to varying concentrations of its target, the protein-electrode combination showed a logarithmically proportional increased resistance to charge transfer from a solution-based redox probe, due to the formation of TLR-4 protein dimers. It also demonstrated excellent sensitivity to trace levels of Gram-negative bacteria, while remaining insensitive to both Gram-positive and viral challenges. Further characterization of our mSAM revealed that maintaining the appropriate receptor orientation on the electrode surface, mimicking TLR-4′s role in a cellular context, was essential in producing a responsive sensor.

1. Introduction

The current standard in the diagnosis of infections relies on slow, cell culture-based methodologies (Bloos, 2015). The time taken to correctly diagnose a serious infection is often detrimental to the patient, yet if the infection is treated aggressively with broad-spectrum antibiotics, this can create future susceptibility to more resistant strains (Bloos, 2015; Neu, 1992). Slow diagnoses are also a detriment to preventing virulent pathogen spread, such as in the case of biological terrorism or warfare, which is a concern for public safety (Kirsch et al., 2013; Lim et al., 2005). For this reason, rapid and accurate identification of infectious agents is needed. Biosensors have emerged as one of the leading technologies for the detection of analytes of biological importance, either as stand-alone devices or as part of a biochip that can detect multiple analytes simultaneously (Daniels and Pourmand, 2007; Gomez et al., 2001; Gooding, 2008; Grow et al., 2003; Koo et al., 2009; Stokes et al., 2001; Vo-Dinh et al., 2003; Yang and Bashir, 2008).

In order to develop the appropriate biosensor to meet this objective, we have chosen to take advantage of the well-characterized pathogen-sensing interaction between the complex of Toll-Like Receptor-4 (TLR-4) and lymphocyte antigen 96 (MD-2) with a Gram-negative bacterial membrane component, lipopolysaccharide (LPS) (Park et al., 2009). TLR-4 and MD-2, hereafter referred to as TLR-4, are part of the human innate immune system and are responsible for triggering the initial response when a Gram-negative infection is identified (Beutler, 2000; Park et al., 2009). A significant advantage of using TLR-4 in this work, as opposed to antibodies, is that TLR-4 recognizes a broad array of LPS moieties, whereas the specificity of antibodies is a hindrance in a sensor that should respond to any and all Gram-negative organisms. Also, as Gram-negative bacteria constantly shed LPS into their environment, LPS is an attractive target for detection (Heumann et al., 2003; Mattsby-Baltzer et al., 1991). Utilizing electrochemistry, we have incorporated this biological interaction into a functional sensor that can help inform clinicians.

Impedance spectroscopy is frequently utilized in biosensing, due to its simplicity, excellent sensitivity, and amenability to miniaturization and multiplexing (Daniels and Pourmand, 2007; Gomez et al., 2001; Reddy et al., 2016; Yang and Bashir, 2008). Several groups have developed impedance-based sensors by tethering probe molecules to electrode surfaces and detecting changes in resistance that depend on the concentration of target molecules, in both biosensors and biochips (Amini et al., 2014; Chen et al., 2008; Ding et al., 2007; Gomez et al.,

* Corresponding author.
E-mail address: birss@ucalgary.ca (V.I. Birss).

http://dx.doi.org/10.1016/j.bios.2016.09.009
Received 17 June 2016; Received in revised form 20 August 2016; Accepted 1 September 2016
Available online 07 September 2016
0956-5663/

2001; Reddy et al., 2016; She et al., 2015; Wang et al., 2015; Yang and Bashir, 2008; Yang et al., 2015). However, a challenge associated with this approach is to effectively tether the capture probe to the surface to reproducibly recognize its target in solution.

Self-assembled monolayers (SAMs) are sulfur-terminated ordered structures (Canaria et al., 2006; Gronbeck et al., 2000; Love et al., 2005) that are frequently used in impedance-based biosensors (Amini et al., 2014; Ding et al., 2007; She et al., 2015). The synthesis of modified SAMs (mSAMs) can be achieved by the chemical modification of a SAM once it is bound, typically to Au (Nicosia and Huskens, 2014). Electrochemical SAM-based sensors have also been shown to be easily miniaturized and commercialized for diagnostic applications, making them an attractive tool for a sensor targeting LPS (Gau et al., 2005; Pan et al., 2010). In the present work, we utilize a surface-modified SAM monolayer to tether the LPS-probe molecule, TLR-4, to a Au electrode in a controlled orientation, in order to optimize recognition and selective binding to its target. LPS detecting sensors involving immobilized functional moieties have been reported previously, including polymyxin B (Abdul Rahman et al., 2013; Ding et al., 2007; Iijima et al., 2011; Kato et al., 2007) and aptamers (Kim et al., 2012; Su et al., 2012, 2013), which were chosen for their LPS selectivity.

While these sensors are quite promising, their response time and specificity, as well as the limit of detection of bacterial cells, have been questionable. TLR-4 was also previously utilized in a biosensor in which the protein was immobilized on a Au microelectrode via a SAM, although it was not tested with bacterial cells or with controls, such as viral particles (Yeo et al., 2011). We have built upon this approach by controlling the orientation of TLR-4 on the electrode surface in order to mimic the conformation on the surface of a cell, and by using a mixture of SAMs of varying length to provide better access of a solution-based redox active species to the underlying Au (Fig. 1). By combining a naturally evolved sensing moiety, i.e., TLR-4, with the speed and portability of well-defined electrochemical techniques, we have designed a sensor which mimics the response and selectivity of the immune system for the detection of LPS (and thus Gram-negative bacteria) over a biologically relevant range of concentrations, including the detection of trace quantities of Gram-negative bacteria.

1.1. Sensor design strategy

For the first layer of our modified SAM (mSAM) (Fig. 1A, single or mixed component SAM, referred to as Layer 1), we utilized a thiol-containing carboxylic acid, 11-mercaptoundecanoic acid (MUA) (Canaria et al., 2006; Gronbeck et al., 2000; Love et al., 2005). We explored SAM designs involving short spacer thiols to lower the overall impedance of the SAMs to levels tolerable by handheld electrochemical instruments, which generally have input impedances that cannot handle the high resistances caused by some SAMs. For our mixed SAMs, the carboxylic acids were spaced using a 9:1 molar ratio of a small spacer thiol, 1-propanethiol, to a 11-carbon carboxylate alkanethiol.

The carboxyl group attached to the end of the immobilized 11-carbon thiol that is exposed to solution was then activated to allow the formation of amide bonds (Bonroy et al., 2006; Witt and Klajn, 2004). This allowed us to tether well-characterized nitrilotriacetic acid (NTA) (Fig. 1A, Layer 2) to the modified electrode surface through the amide bond (Han et al., 2006; Kröger et al., 1999). By then complexing Ni^{2+} to NTA (Fig. 1A, Layer 3), the Ni-NTA functionalized surface can effectively bind proteins that have a poly-histidine tag, such as the recombinant TLR-4 used in this work (Han et al., 2006; Hochuli et al., 1987; Kröger et al., 1999). This then allowed the attachment of poly-histidine tagged proteins (Fig. 1B, Layer 4), e.g., TLR-4, to the electrode surface in an ordered manner.

The mode of action by which TLR-4 binds to LPS in vivo is through dimerization (Beutler, 2000; Park et al., 2009), where two TLR-4 molecules transiently interact to trap two LPS molecules. We propose a model in which dimerization of proximal TLR-4s and the binding of the macromolecular LPS will modulate the access of redox ions to the underlying Au (Fig. 1C). As LPS binds to the TLR-4 moieties on the electrode surface, access by probe redox ions in solution to the Au should be inhibited, as they can only oxidize/reduce at defects within the mSAM layer (Campuzano et al., 2006; Diao et al., 2001; Han et al., 2006).

Through the presence of the probe ion in solution, specifically Fe^{3+}, the impedance of our sensor was monitored in a rapid and quantifiable manner. As more LPS was selectively bound to the TLR-4 groups on the electrode, the access to the underlying Au was further restricted, generating a gradually increasing impedance with increasing LPS concentration in solution. It was shown that the model proposed above (Fig. 1) leads to impedance changes that reflect the predicted TLR-4/LPS interactions, providing a method of monitoring LPS, and hence Gram-negative bacteria, in a sample.

2. Experimental methods

2.1. Equipment and Electrodes

A standard three-electrode setup was used in conjunction with a Bio-Logic SP-300 potentiostat with an ultra-low current cable and impedance module for all electrochemical experiments, with the data being collected by the EC-Lab software (version 10.37). All experiments were performed inside a Faraday cage, with the exception of the Au cleaning steps. All water used in this work was triply distilled prior to use and all experiments were performed at room temperature.

Au electrodes were purchased from Deposition Research Laboratories as sputtered glass slides with a 40 nm Ti adhesion layer and 100 nm of Au on top and then cut with a diamond saw to expose a consistent 5×10 mm area of Au. The electrodes were rinsed in acetone, isopropanol, ethanol, and finally in water before being electrochemically cleaned in unstirred 0.5 M H_2SO_4 (EMD Millipore, ACS grade), deaerated with nitrogen gas for 20 min prior to cleaning. For the electrochemical cleaning, a three electrode setup was used with a Pt mesh counter electrode (CE) and a reversible hydrogen reference electrode (RHE). The Au electrode was electrically connected to a Cu clip that remained suspended above the solution. The potential of the Au electrode was scanned between 0.05 and 1.7 V vs RHE at a sweep rate of between 100 and 500 mV/s until the CVs gave the characteristic response of Au.

In other experiments, a Au micro-disc electrode with a diameter of 0.5 mm (area of 0.002 cm^2) was used and contacted via a NiCr wire. The microelectrode was cleaned, modified, and tested following the same procedures described above for the larger Au electrodes.

2.2. SAM deposition and Testing

Self-assembled monolayers (SAMs) were formed on clean Au by submerging them in 10 mL ethanolic solutions of 10 mM thiol for 24 h. 11-Mercaptoundecanoic acid (MUA, Sigma-Aldrich, 95% purity) was dissolved in ethanol (Sigma-Aldrich, 99% purity) to the desired concentration, while 1-propanethiol (Sigma-Aldrich, 99% purity) was diluted in ethanol. For mixed SAM construction, 1-propanethiol was diluted to 9 mM and combined with 1 mM MUA, achieving a total thiol concentration of 10 mM. After thiol attachment, the electrodes were rinsed sequentially with ethanol followed by water before being evaluated electrochemically, using a Pt mesh CE and an Ag/AgCl reference electrode.

5 mM of the sodium salt of ferric ethylenediaminetetraacetic acid (Fe-EDTA, Sigma-Aldrich, BioReagent grade) or a 5 mM potassium ferri/ferrocyanide redox couple were used as the redox probe. All EIS experiments were performed at the $E^{0'}$ of these Fe(II/III) couples, determined by cyclic voltammetry using a Pt microelectrode before each EIS experiment. The $E^{0'}$ value was always sufficiently positive (>

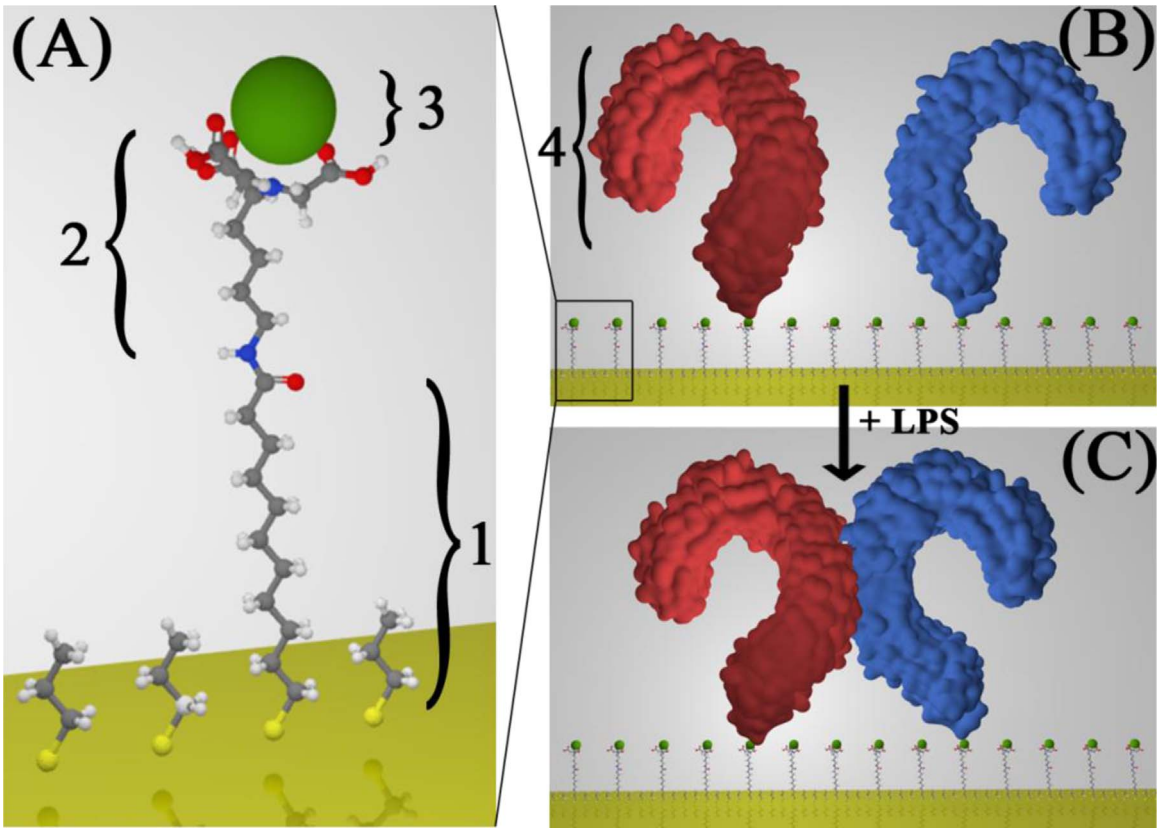

Fig. 1. (A) Schematic of modified SAM (mSAM) capable of immobilizing poly-histidine tagged proteins, such as TLR-4. Layer 1 is a mixed SAM of short and long alkanethiols attached to Au through a sulfur linkage, while Layer 2 consists of a nitrilotriacetic acid (NTA) group that can coordinate Ni^{2+} ions (Layer 3). (B) Schematic representation of the sensor bonded to TLR-4 (Layer 4), where the TLR-4 structure is adapted from the PDB file 3FXI. (C) Diagram showing how binding of LPS to TLR-4 causes a dimerization event that limits probe ion access to underlying Au.

0.1 V vs SHE for all Fe species tested) to avoid Ni^{2+} (part of the mSAM shown in Fig. 1) reduction ($E^{0'}$=−0.28 V vs SHE). The supporting electrolyte was 25 mL of 0.2 M pH 7 phosphate buffer solution that was vigorously bubbled with N_2 for 20 min to deaerate the cell solution prior to testing, after which N_2 was passed continuously over the solution surface.

2.3. Modified self assembled monolayer (mSAM) construction

The terminal COOH groups of 11-mercaptoundecanoic acid were activated by submerging the SAM-modified electrode in a solution of 2 mg 1-ethyl-3-(3-dimethylaminopropyl)carbodiimide (EDC, Sigma-Aldrich, 99% purity), 5.5 mg N-hydroxysuccinimide (NHS, Sigma-Aldrich, 98% purity), and 0.108 g 4-morphilineethanesulfonic acid (MES, Sigma-Aldrich, Biotechnology grade) in 5 mL of water for one hour under constant N_2. Following the activation of the COOH groups, the electrode was submerged in 10 mL of 1 mM N_α,N_α-bis(carboxymethyl)-L-lysine (Sigma-Aldrich, 97% purity) at 4 °C for 24 h. The electrode was then rinsed with water and soaked in 10 mL of 0.1 M $NiSO_4$ for 15 min before being rinsed with water again. It was then submerged in a 1 mL 5 μg/mL solution of purified recombinant human TLR-4/MD-2 with a 10x His-tag (extracellular N-terminal fragment, R & D Systems, USA, carrier-free) for 15 min, followed by another rinse with water.

After each new layer of the mSAM (Fig. 1a) was deposited, the electrode was tested electrochemically using the same protocol as used in the electrochemical experiments after SAM deposition, described above. The mSAM construction was tracked via contact angle measurements with drops of triply distilled water and a PHI VersaProbe 5000 X-ray photoelectron spectroscopy instrument to track the O1s spectra at Layers 1–4.

2.4. Sensor testing and equivalent circuit fitting

TLR-4 modified electrodes were exposed to concentrations of lipopolysaccharide (LPS, Sigma-Aldrich, serotype O127: B8, phenol extracted) from 1 ng/mL to 10 μg/mL using the electrochemical methodology described above. The LPS was added to the cell via a micropipette and using concentrated stocks, and the cell solution was then mixed vigorously with a micropipette before being allowed to interact with the electrode for 20 min under N_2 prior to electrochemical testing. The EIS response at the $E^{0'}$ of the Fe-EDTA or ferri/ferrocyanide redox couple was recorded (10 mV rms amplitude and between 1 MHz and 10 mHz, sweeping in both directions) and the data were then best-fitted to an equivalent circuit in order to obtain a good estimate of the resistance across the interface. The EC-Lab software was used to approximate a fit and the resistance at each concentration of LPS was compared to the baseline levels for that electrode.

For the determination of the sensor response to Gram-positive or Gram-negative organisms, the electrodes were fabricated as described above and exposed to either heat killed *Salmonella typhimurium* (Invivogen) or *Staphylococcus aureus* (Invivogen) at concentrations ranging from 10^0 cells/mL to 10^5 cells/mL. These concentrations were determined from serially diluted stock solutions stored at −20 °C. All stock solutions of bacteria were thoroughly mixed prior to dilution to ensure homogeneity. Viral tests were conducted with UV-inactivated *Rhabdovirus* from an in-house preparation at 10^4 and 10^5 viral particles/mL (Cumming School of Medicine, University of Calgary).

3. Results and discussion

3.1. Construction and evaluation of TLR-4 modified SAM response to LPS

It has been shown that alkanethiols with short chain lengths (e.g., propanethiol) exhibit a lower impedance when deposited as a self-assembled monolayer (SAM) on Au than longer alkanethiols, such as 11-mercaptoundecanoic acid (MUA) (Campuzano et al., 2006). Many groups have previously shown that a SAM composed of a mixture of two different thiols is capable of binding proteins with a poly-histidine tag, similar to the one found on TLR-4 (Bonroy et al., 2006; Rickert et al., 1996). Based on this concept of using shorter thiols as low-impedance "spacers" between longer-chain, more resistive thiols, we deposited a mixture of MUA and 1-propanethiol (C3), followed by the addition of the Ni-NTA and TLR-4 layers, as described in Section 2.3, as a strategy to lower the overall impedance of the final modified SAM (mSAM) and to thus facilitate sensing.

The contact angle was tracked throughout mSAM deposition and the hydrophilicity of the surface was seen to increase as each new layer was attached (Fig. S1), as expected, due to the addition of COOH groups in Layer 2 and the hydrophilic protein in Layer 4. The oxygen content of the mSAM, which should increase with subsequent layers, was also seen to increase via X-ray photoelectron spectroscopy throughout the mSAM deposition (Fig. S2). These results thus offer some confirmation that the desired surface modifications were achieved in each sensor layer fabrication step.

As can be seen in Fig. 2A, the addition of LPS to the solution results in a rapid increase in the electrode impedance that is proportional to the amount of LPS added to the solution. This is proposed to be due to the dimerization of TLR-4 around the LPS target, bridging the MUA-based mSAMs above the C3 spacers (Fig. 1A) and effectively decreasing the size of these channels, as proposed in Fig. 1C. This lowers the overall rate of electron tunneling through the C3 thiols, thus increasing the measured resistance. If the dimerization process had resulted in opening of pores in the mSAM, the impedance would have decreased, which was not seen in this work.

Fig. 2B shows the response of three different sensors, constructed using the 9:1 molar ratio of the C3 thiol: MUA, to LPS over a biologically relevant range of concentrations. Some fluctuation in the baseline resistance (no LPS present) of the TLR-4 modified mSAMs was observed between sensors, which may be related to some variations in the Au electrode (0.5 cm^2 area) surface properties and/or in the SAM structure/composition (Love et al., 2005). Importantly, however, the increase in the impedance relative to the baseline impedance obtained from the TLR-4 modified SAM without any LPS in solution for each sensor was reproducible, indicating that the sensor could be used in practice by employing methods such as standard addition, where a known concentration of LPS is added to the sample after it has been analyzed (Akyilmaz et al., 2003; Li et al., 1999; Liu et al., 2003, 2005; Yang et al., 2006). This is in line with many current analytical techniques and could be easily adapted for diagnostic use.

Also, in order to prepare for the use of our LPS sensor in practice, potentially using microelectrode arrays, the mSAM was deposited on a Au microelectrode (with a geometric area of 0.002 cm^2) and then tested for its response to LPS. The response shown in Fig. S3 is seen to be similar to the larger area electrodes used in Figs. 2 and 3, demonstrating the robustness of this system towards miniaturization.

3.2. Inactive organism testing for sensitivity and specificity

While sensing LPS in solution provides a proof-of-principle for our TLR-4 sensor, as LPS is shed specifically by Gram-negative bacteria (Heumann et al., 2003; Mattsby-Baltzer et al., 1991), the detection of Gram-negative bacteria is more clinically relevant. As such, we exposed our sensor to varying concentrations of the Gram-negative organism *Salmonella typhimurium*. As shown in Fig. 3A, additions of *Salmonella* resulted in an increase in the measured resistance, similar to what is seen for increasing solution concentrations of purified LPS (Fig. 2B), with the minimum concentration for detection of heat-killed *Salmonella* being ca. 10^0 cells/mL. As the preparation of these cells involves lysis, LPS should have been released, with an expected 10^5 molecules of LPS on each bacterial cell (Smit et al., 1975).

Because of the complexity of biological samples, it was considered possible that the higher impedance observed when LPS was added was caused by nonspecific adsorption of macromolecules released from the Gram-negative bacteria rather than the high level of LPS in solution. To test this hypothesis, we performed control experiments using Gram-positive bacteria and viruses (Fig. 3B and C). When exposed to the Gram-positive bacterium *Staphylococcus aureus* at the high concentrations of 10^4 and 10^5 cells/mL, the sensor showed complete insensitivity (Fig. 3B), as these bacteria do not produce surface LPS and therefore should not elicit a response from TLR-4. The same trend was also observed when the TLR-4 modified mSAMs were exposed to similar concentrations of viral particles, as shown in Fig. 3C. If nonspecific adsorption was indeed occurring and had caused the impedance to increase, this should also have been observed in the control experiments. However, the control bacteria and viruses did not affect the measured signal (Fig. 3B and C), indicating that the increase of R_p with increasing bacteria (10^5 LPS/cell) and LPS concentration is not due to nonspecific adsorption effects. Coupled with the response obtained from low concentrations of the Gram-negative *Salmonella* in solution, this indicates that this sensor design has potential for the detection of Gram-negative bacteria.

3.3. Insights into mechanism of LPS sensing by TLR-4 modified electrodes

The mSAM/TLR-4 modified electrodes respond to LPS or bacteria in a logarithmic fashion (Fig. 2B), similar to what has been reported previously during impedance-based sensing of a number of other soluble targets (Chen et al., 2008; Yang et al., 2015). A logarithmic LPS-TLR-4 interaction could indicate that the sensing mechanism involves surface adsorption with lateral interactions between the attached surface moieties, e.g., a Temkin isotherm (Johnson and Arnold, 1995). If such an isotherm applies to the mSAM/TLR-4 sensor, then as more LPS is bound onto the surface, the equilibrium constant defining the binding of LPS to TLR-4 would decrease. This is because repulsive lateral interactions develop between surface LPS groups, i.e., as one pair of TLR-4 molecules binds LPS and dimerizes, the adjacent TLR-4s would lose a potential partner for its own dimerization. Because the mechanism of LPS binding to TLR-4 depends on TLR-4 dimerization, we are unable to determine if the observed increase in impedance with added LPS is due to TLR-4 dimerization, or is due to steric blocking by LPS, as both of these processes would prevent access of the redox probe to the underlying Au substrate.

To further probe the mechanism by which our sensor responds to LPS, we examined the interaction of LPS with the electrode at various stages of construction of the mSAM. Table S1 shows the EIS circuit parameters obtained for bare Au, a SAM composed of a 9:1 molar ratio of propanethiol: MUA, and a Ni-NTA functionalized mSAM, to 10 μg/mL of LPS added to the Fe^{3+}-containing PBS. While the impedance of bare Au did increase slightly with the addition of LPS to the solution, the impedance did not increase when the thiol- or thiol-Ni-NTA layers were exposed to LPS. This indicates that LPS is being sensed only when TLR-4 is present on the mSAM surface.

To determine if TLR-4 alone on Au, without the underlying mSAM, is sufficient to generate a response to LPS, TLR-4 was adsorbed on bare Au by pipetting ca. 100 μL of 5 μg/mL TLR-4 onto the Au surface and allowing the aliquot to dry in air. This was expected to physically adsorb TLR-4 in a random manner on the surface, with no preferred orientation. This should result in a minimal LPS response, as no

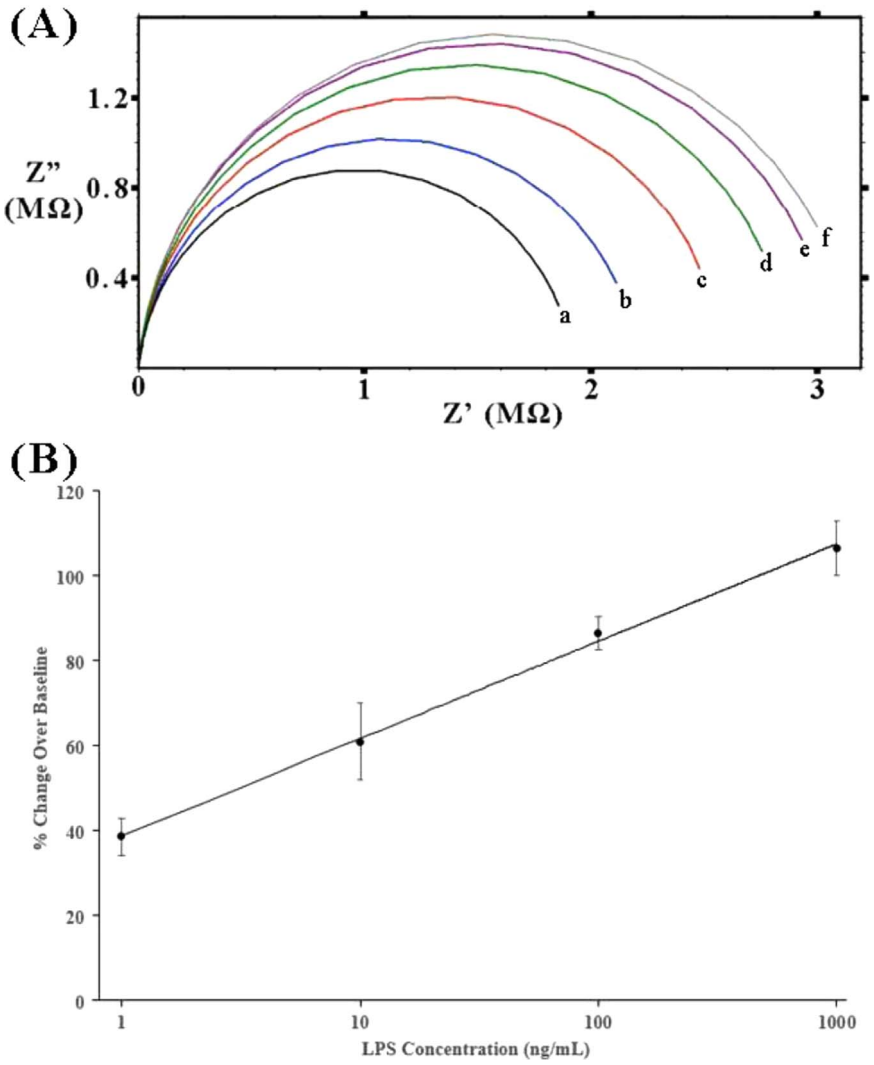

Fig. 2. (A) EIS response of a mSAM-based TLR-4 sensor composed of a 9:1 molar ratio of C3 spacer thiols:MUA on Au sputter-coated glass slides. Trace (a) represents the TLR-4 modified baseline, while trace (b) is for 1 ng/mL of LPS, increasing logarithmically to 10,000 ng/mL of LPS in trace (f). (B) Percent increase in R_p of TLR-4 modified mSAM to LPS relative to the baseline resistance of TLR-4 modified mSAMs with no LPS present. All mSAMs were constructed using a 9:1 molar ratio of C3 spacer:MUA. The data shown are an average of what was obtained from three sensors, with the error bars representing the coefficient of variation. All data were collected at the $E^{o'}$ of the $Fe^{2+/3+}$ couple in 0.2 M pH 7 phosphate buffer.

organized channels should be present to be closed as a result of a TLR-4 dimerization event. As predicted, the EIS response (Fig. 4) was significantly different from the results shown in Fig. 3 for the sensor in which TLR-4 was bound in a controlled orientation on the modified SAM substrate.

First, the EIS spectrum exhibits a significantly lower impedance by several orders of magnitude than seen for TLR-4 bound to the modified SAMs (e.g., Fig. 3), suggesting that the coverage of TLR-4 on the surface is indeed lower in the absence of the underlying layers. This is not surprising, because packing of the TLR-4 proteins in a random orientation would likely be less tight than the ordered on-end orientation obtained when using the Ni^{2+}-NTA SAM (Fig. 1). In the absence of the interaction between Ni^{2+}-NTA and the poly-histidine tag, it is also likely that even gentle rinsing of the surface with buffer solution would cause some of the weakly adsorbed TLR-4 to be removed. The much lower surface resistance may also be observed because the TLR-4 protein exhibits a horseshoe-shaped structure that would result in an open cavity in the centre of the protein that could act as a pinhole for access to the redox active species.

It is also seen that the presence of only physisorbed TLR-4 (Fig. 4) results in two time constants (two arcs in the Nyquist plot), as compared to the single time constant seen for our standard sensors (Figs. 2 and 3). The presence of two time constants could reflect the non-homogenous (disorganized) and stochastic deposition of TLR-4 on the bare Au surface. Another possible explanation for this could be a tightening of some of the pores in a matrix of proteins as neighbouring TLR-4s interact with each other. When exposed to 1 μg/mL LPS, the relative resistance of the two time constants is seen to change, although the total resistance (full diameter including both arcs in Fig. 4) does not increase significantly.

Overall, it is clear that a randomly and weakly adsorbed surface film does not respond reliably to LPS (Fig. 4), as seen for the well-oriented TLR-4 mSAMs in Fig. 2, and that the coverage of TLR-4 is likely much lower. This highlights the critical need for the presence of the modified SAM to serve as a binding layer between TLR-4 and Au, resulting in a higher TLR-4 coverage and ensuring a specific surface orientation.

Although TLR-4, adsorbed directly on Au, does not generate a reliable response to LPS, we also probed the interaction of LPS to TLR-4 that was immobilized to a SAM in a random orientation (Fig. 5A) in comparison to the oriented TLR-4 obtained utilizing the mSAM approach (Fig. 5B). By activating the terminal COOH group of MUA with the EDC/NHS method, described in Section 2.3, and then exposing the electrode to TLR-4 for 24 h at 4 °C, we immobilized TLR-4 to a SAM composed of a 9:1 molar ratio of 1-propanethiol:

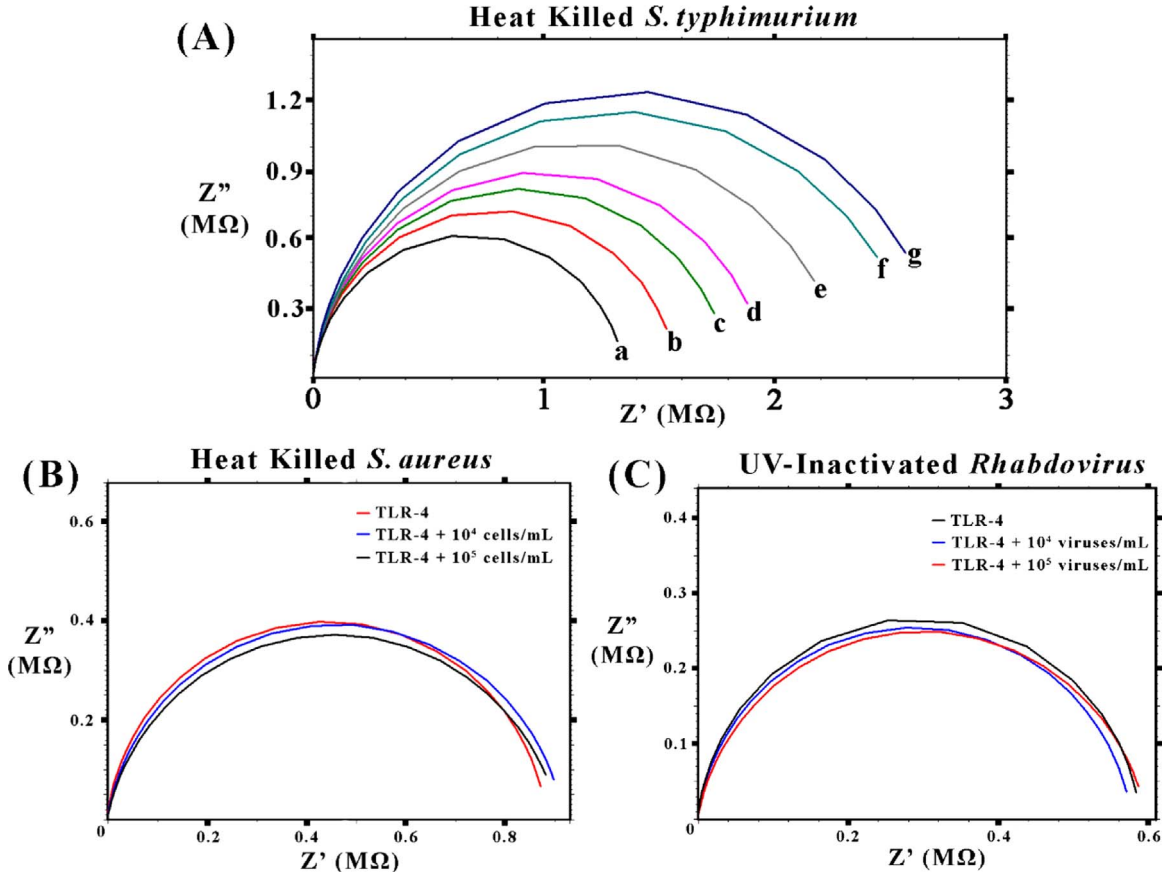

Fig. 3. (A) Representative EIS response to Gram-negative organisms of mSAM-based TLR-4 sensors composed of a 9:1 molar ratio of 1-propanethiol to MUA on Au sputter-coated glass slides. The electrode responds reliably to increasing concentrations of *S. typhimurium*. Trace (a) represents the TLR-4 modified baseline, while trace (b) is for 10^0 cells/mL, increasing logarithmically to 10^5 cells/mL in trace (g). (B and C) Representative EIS response from mSAM-based TLR-4 sensors to (B) Gram-positive organisms and (C) viral organisms. All data were collected at the $E^{0'}$ of $Fe^{2+/3+}$ in 0.2 M pH 7 PBS +5 mM Fe^{3+}-EDTA.

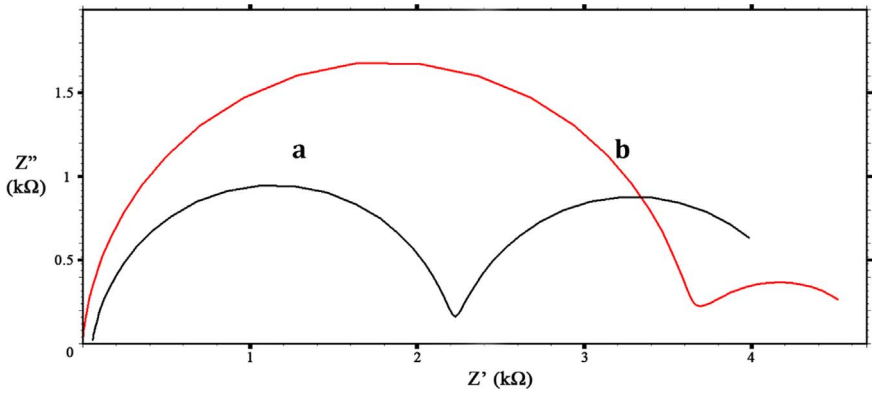

Fig. 4. EIS response of randomly deposited TLR-4 on clean (no SAM) Au sputter-coated glass slides. Trace a represents the EIS response of the electrode in phosphate buffer solution, while trace b was obtained in phosphate buffer that was spiked with 1 μg/mL LPS. All data were collected at the $E^{0'}$ of Fe^{3+} in 0.2 M pH 7 PBS supplemented with 5 mM Fe^{3+}.

MUA. Using this method, any primary amine on the protein could interact with the activated COOH to immobilize the protein, and as there are several amino acids with terminal amines present, it is possible that the different orientations of TLR-4 disable the target recognition domain and prevent TLR-4 dimerization around LPS.

Fig. 5C shows the result of the random immobilization of TLR-4 to a 9:1 molar ratio of C3: MUA SAM on Au, without the TLR-4-ordering offered by the Ni-NTA layer. Compared to the oriented mSAM/TLR-4 sensors, the response to LPS is relatively weak and is not correlated with the LPS concentration (Fig. 5C). Similar results, where an orientated probe protein provides a larger response than a randomly oriented control, have been reported previously (Bonroy et al., 2006). The results in Fig. 4 and the fact that the Ni^{2+}-NTA layer itself does not respond well to LPS (Table S1) thus indicate that a modified SAM, capable of orienting TLR-4 on the surface, is essential for the optimal performance of our TLR-4 based sensor.

4. Conclusions

We have successfully developed an orientation-specific biosensor that utilizes Toll-Like Receptor-4 (TLR-4) to detect the presence of Gram-negative bacteria. This sensor is based on a modified self-assembled monolayer (mSAM), consisting of a mixed thiol SAM, modified at the solution end with a Ni^{2+}-nitrilotriacetic acid functional group that binds selectively to the his-tag of TLR-4 such that the ligand binding domains are consistently oriented towards the solution. This

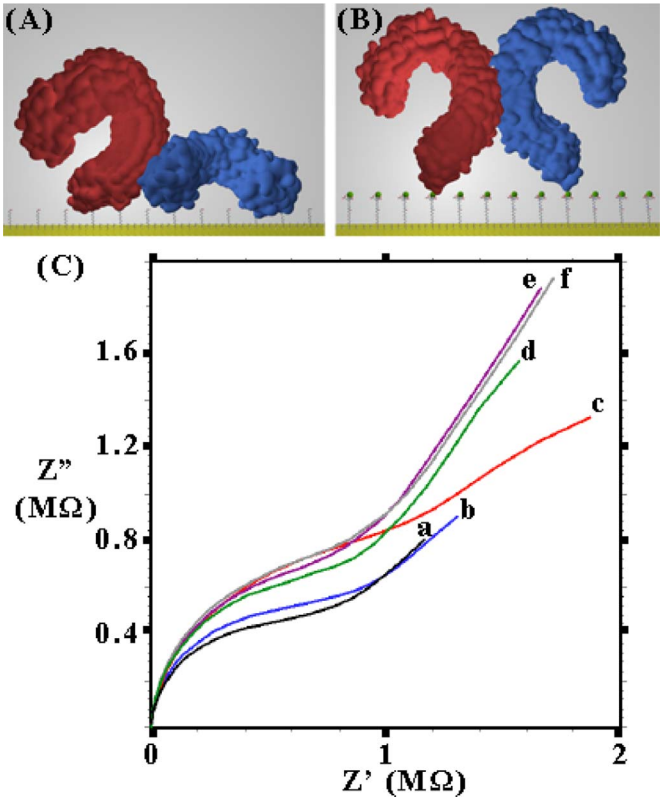

Fig. 5. (A) Schematic of random adsorption of TLR-4 onto a SAM-modified electrode via amide bonds, in comparison with (B), which shows the orientated tethering of TLR-4 onto a mSAM, both on Au sputter-coated glass slides. (C) EIS data obtained for a randomly oriented TLR-4 on a SAM modified electrode versus the TLR-4 baseline (trace a) when exposed to increasing concentrations of LPS from (b-f) 1, 10, 100, 1,000, and 10,000 ng/mL LPS. All data were collected at the $E^{0'}$ of $Fe^{2+/3+}$ in 0.2 M pH 7 PBS supplemented with 5 mM Fe^{3+}.

approach has taken advantage of a mixture of both short (3 carbons) spacer thiols and longer derivatizable thiols (11 carbons) to increase the number of solution-accessible channels in the mSAM. Our hypothesis was that, when TLR-4 interacts with lipopolysaccharide (LPS) in solution, the protein would dimerize, thus effectively closing the channels to a $Fe^{2+/3+}$ redox probe in the solution.

In support of this, it was found that a reproducible, dose-dependent, logarithmic increase in the electrochemical impedance of the modified Au was observed, using both Au sputter-coated glass slides and miniaturized Au microelectrodes. When challenged with non-target organisms, such as Gram-positive bacteria or a virus, the TLR-4 based sensor gave no response. However, Gram-negative bacteria elicited a larger response than LPS alone, providing resolution to levels approximating 10^0 cells/mL (ca. 10^5 LPS molecules on each bacterial cell). This work represents the first experiments of this kind for a TLR-4 based biosensor, specifically utilizing organisms instead of purified components and showing that non-target organisms do not elicit any response from the sensor. It was also shown that the sensor response is highly dependent on the surface orientation of the bound TLR-4, as randomly adsorbed proteins, attached either directly to Au or to the SAMs, failed to generate a similarly useful response.

Our work demonstrates the utility of a Toll-Like Receptor biosensor for the detection of Gram-negative bacteria. When coupled with a testing protocol, such as standard addition, this sensor could become a useful diagnostic tool. This is of interest in the diagnosis of conditions, such as sepsis, where normally sterile blood is infected with bacteria, or for pathogen identification, which is a major concern for public safety amid the growing threat of bioterrorism. As this model depends solely on the dimerization of the TLR-4 protein, this sensing strategy could theoretically be applied to any protein-ligand interactions involving dimer formation, including other immune system receptors.

Acknowledgements

The authors gratefully acknowledge Defence Research and Development Canada (contract # is W7702-145656/A) for the support of this work and for providing direction for the project, the Natural Sciences and Engineering Research Council of Canada for funding of equipment and lab facilities, and the Vanier Canada Graduate Scholarship and Alberta Innovates Technology Futures Graduate Student Scholarship programs for supporting RMM. UV-inactivated *Rhabdovirus* was graciously provided by Drs. Doug Mahoney and Paul Kubes at the University of Calgary.

Appendix A. Supporting information

Supplementary data associated with this article can be found in the online version at doi:10.1016/j.bios.2016.09.009.

References

Abdul Rahman, M.S., Mukhopadhyay, S.C., Yu, P.L., Goicoechea, J., Matias, I.R., Gooneratne, C.P., Kosel, J., 2013. Detection of bacterial endotoxin in food: New planar interdigital sensors based approach. J. Food Eng. 114, 346–360. http://dx.doi.org/10.1016/j.jfoodeng.2012.08.026.

Akyilmaz, E., Sezgintürk, M.K., Dinçkaya, E., 2003. A biosensor based on urate oxidase-peroxidase coupled enzyme system for uric acid determination in urine. Talanta 61, 73–79. http://dx.doi.org/10.1016/S0039-9140(03)00239-X.

Amini, K., Chan, N.W.C., Kraatz, H.-B., 2014. Toll-Like Receptor 3 modified Au electrodes: an investigation into the interaction of TLR3 immobilized on Au surfaces with poly(I: C). Anal. Methods 6, 3322. http://dx.doi.org/10.1039/c4ay00369a.

Beutler, B., 2000. Tlr4: Central component of the sole mammalian LPS sensor. Curr. Opin. Immunol. 12, 20–26. http://dx.doi.org/10.1016/S0952-7915(99)00046-1.

Bloos, F., 2015. Clinical diagnosis of sepsis and the combined use of biomarkers and culture- and non-culture-based assays. In: Mancini, N. (Ed.), Sepsis: Diagnostic Methods and Protocols, 247–260. http://dx.doi.org/10.1007/978-1-4939-1776-1.

Bonroy, K., Frederix, F., Reekmans, G., Dewolf, E., De Palma, R., Borghs, G., Declerck, P., Goddeeris, B., 2006. Comparison of random and oriented immobilisation of antibody fragments on mixed self-assembled monolayers. J. Immunol. Methods 312, 167–181. http://dx.doi.org/10.1016/j.jim.2006.03.007.

Campuzano, S., Pedrero, M., Montemayor, C., Fatás, E., Pingarrón, J.M., 2006. Characterization of alkanethiol-self-assembled monolayers-modified gold electrodes by electrochemical impedance spectroscopy. J. Electroanal. Chem. 586, 112–121. http://dx.doi.org/10.1016/j.jelechem.2005.09.007.

Canaria, C. a, So, J., Maloney, J.R., Yu, C.J., Smith, J.O., Roukes, M.L., Fraser, S.E., Lansford, R., 2006. Formation and removal of alkylthiolate self-assembled monolayers on gold in aqueous solutions. Lab Chip 6, 289–295. http://dx.doi.org/10.1039/b510661c.

Chen, W., Lu, Z., Li, C.M., 2008. Sensitive human interleukin 5 impedimetric sensor based on polypyrrole-pyrrolepropylic acid-gold nanocomposite. Anal. Chem. 80, 8485–8492. http://dx.doi.org/10.1021/ac8012225.

Daniels, J.S., Pourmand, N., 2007. Label-free impedance biosensors: Opportunities and challenges. Electroanalysis 19, 1239–1257. http://dx.doi.org/10.1002/elan.200603855.

Diao, P., Guo, M., Tong, R., 2001. Characterization of defects in the formation process of self-assembled thiol monolayers by electrochemical impedance spectroscopy. J. Electroanal. Chem.. http://dx.doi.org/10.1016/S0022-0728(00)00424-1.

Ding, S.J., Chang, B.W., Wu, C.C., Chen, C.J., Chang, H.C., 2007. A new method for detection of endotoxin on polymyxin B-immobilized gold electrodes. Electrochem. Commun. 9, 1206–1211. http://dx.doi.org/10.1016/j.elecom.2006.12.029.

Gau, V., Ma, S., Wang, H., Tsukuda, J., Kibler, J., Haake, D.A., 2005. Electrochemical molecular analysis without nucleic acid amplification. Methods 37, 73–83. http://dx.doi.org/10.1016/j.ymeth.2005.05.008.

Gomez, R., Bashir, R., Sarikaya, A., 2001. Microfluidic biochip for impedance spectroscopy of biological species. Biomed. Microdevices 3, 201–209. http://dx.doi.org/10.1023/A:1011403112850.

Gooding, J.J., 2008. Advances in interfacial design for electrochemical biosensors and sensors: Aryl diazonium salts for modifying carbon and metal electrodes. Electroanalysis 20, 573–582. http://dx.doi.org/10.1002/elan.200704124.

Gronbeck, H., Curioni, A., Andreoni, W., 2000. Thiols and disulfides on the Au (111) surface: the headgroup – gold interaction. J. Am. Chem. Soc. 122, 3839–3842. http://dx.doi.org/10.1021/ja993622x.

Grow, A.E., Wood, L.L., Claycomb, J.L., Thompson, P.A., 2003. New biochip technology for label-free detection of pathogens and their toxins. J. Microbiol. Methods 53, 221–233. http://dx.doi.org/10.1016/S0167-7012(03)00026-5.

Han, A., Takarada, T., Shibata, T., Nakayama, M., Maeda, M., 2006. A MutS protein-immobilized au electrode for detecting single-base mismatch of DNA. Anal. Sci. 22, 663–666. http://dx.doi.org/10.2116/analsci.22.663.

Heumann, D., Lauener, R., Ryffel, B., 2003. The dual role of LBP and CD14 in response

to Gram-negative bacteria or Gram-negative compounds. J. Endotoxin Res. 9, 381–384. http://dx.doi.org/10.1179/096805103225003312.
Hochuli, E., Döbeli, H., Schacher, a, 1987. New metal chelate adsorbent selective for proteins and peptides containing neighbouring histidine residues. J. Chromatogr. 411, 177–184. http://dx.doi.org/10.1016/S0021-9673(00)93969-4.
Iijima, S., Kato, D., Yabuki, S., Niwa, O., Mizutani, F., 2011. Enzymatically amplified electrochemical detection for lipopolysaccharide using ferrocene-attached polymyxin B and its analogue. Biosens. Bioelectron. 26, 2080–2084. http://dx.doi.org/10.1016/j.bios.2010.09.009.
Johnson, R.D., Arnold, F.H., 1995. The Temkin isotherm describes heterogeneous protein adsorption. Biochim. Biophys. Acta – Protein Struct. Mol. Enzym. 1247, 293–297. http://dx.doi.org/10.1016/0167-4838(95)00006-G.
Kato, D., Iijima, S., Kurita, R., Sato, Y., Jia, J., Yabuki, S., Mizutani, F., Niwa, O., 2007. Electrochemically amplified detection for lipopolysaccharide using ferrocenylboronic acid. Biosens. Bioelectron. 22, 1527–1531. http://dx.doi.org/10.1016/j.bios.2006.05.020.
Kim, S.E., Su, W., Cho, M., Lee, Y., Choe, W.S., 2012. Harnessing aptamers for electrochemical detection of endotoxin. Anal. Biochem. 424, 12–20. http://dx.doi.org/10.1016/j.ab.2012.02.016.
Kirsch, J., Siltanen, C., Zhou, Q., Revzin, A., Simonian, A., 2013. Biosensor technology: recent advances in threat agent detection and medicine. Chem. Soc. Rev. 42, 8733–8768. http://dx.doi.org/10.1039/c3cs60141b.
Koo, O.K., Liu, Y., Shuaib, S., Bhattacharya, S., Ladisch, M.R., Bashir, R., Bhunia, A.K., 2009. Targeted capture of pathogenic bacteria using a mammalian cell receptor coupled with dielectrophoresis on a biochip. Anal. Chem. 81, 3094–3101. http://dx.doi.org/10.1021/ac9000833.
Kröger, D., Liley, M., Schiweck, W., Skerra, A., Vogel, H., 1999. Immobilization of histidine-tagged proteins on gold surfaces using chelator thioalkanes. Biosens. Bioelectron. 14, 155–161. http://dx.doi.org/10.1016/S0956-5663(98)00116-X.
Li, J., Chia, L.S., Goh, N.K., Tan, S.N., 1999. Renewable silica sol-gel derived carbon composite based glucose biosensor. J. Electroanal. Chem. 460, 234–241. http://dx.doi.org/10.1016/S0022-0728(98)00381-7.
Lim, D.V., Simpson, J.M., Kearns, E. a, Kramer, M.F., Lim, D.V., Simpson, J.M., Kearns, E. a, Kramer, M.F., 2005. Current and developing technologies for monitoring agents of bioterrorism and biowarfare current and developing technologies for monitoring agents of bioterrorism and biowarfare. Clin. Microbiol. Rev. 18, 583–607. http://dx.doi.org/10.1128/CMR.18.4.583.
Liu, B., Cao, Y., Chen, D., Kong, J., Deng, J., 2003. Amperometric biosensor based on a nanoporous ZrO_2 matrix. Anal. Chim. Acta 478, 59–66. http://dx.doi.org/10.1016/S0003-2670(02)01480-0.
Liu, Z., Liu, Y., Yang, H., Yang, Y., Shen, G., Yu, R., 2005. A phenol biosensor based on immobilizing tyrosinase to modified core-shell magnetic nanoparticles supported at a carbon paste electrode. Anal. Chim. Acta 533, 3–9. http://dx.doi.org/10.1016/j.aca.2004.10.077.
Love, J.C., Estroff, L.A., Kriebel, J.K., Nuzzo, R.G., Whitesides, G.M., 2005. Self-assembled monolayers of thiolates on methals as a form of nanotechnology. Chem. Rev..
Mattsby-Baltzer, I., Lindgren, K., Lindholm, B., Edebo, L., 1991. Endotoxin shedding by enterobacteria: Free and cell-bound endotoxin differ in Limulus activity. Infect. Immun. 59, 689–695.
Neu, H.C., 1992. The crisis in antibiotic resistance. Science 257, 1064–1073. http://dx.doi.org/10.1126/science.257.5073.1064.
Nicosia, C., Huskens, J., 2014. Reactive self-assembled monolayers: from surface functionalization to gradient formation. Mater. Horiz. 1, 32. http://dx.doi.org/10.1039/c3mh00046j.
Pan, Y., Sonn, G. a, Sin, M.L.Y., Mach, K.E., Shih, M.-C., Gau, V., Wong, P.K., Liao, J.C., 2010. Electrochemical immunosensor detection of urinary lactoferrin in clinical samples for urinary tract infection diagnosis. Biosens. Bioelectron. 26, 649–654. http://dx.doi.org/10.1016/j.bios.2010.07.002.
Park, B.S., Song, D.H., Kim, H.M., Choi, B.-S., Lee, H., Lee, J.-O., 2009. The structural basis of lipopolysaccharide recognition by the TLR4-MD-2 complex. Nature 458, 1191–1195. http://dx.doi.org/10.1038/nature07830.
Reddy, B., Salm, E., Bashir, R., 2016. Electrical Chips for Biological Point-of-Care Detection. Annu. Rev. Biomed. Eng. 18, 329–355. http://dx.doi.org/10.1146/annurev-bioeng-071813-104643.
Rickert, J., Göpel, W., Beck, W., Jung, G., Heiduschka, P., 1996. A “mixed” self-assembled monolayer for an impedimetric immunosensor. Biosens. Bioelectron. 11, 757–768. http://dx.doi.org/10.1016/0956-5663(96)85927-6.
She, Z., Topping, K., Shamsi, M.H., Wang, N., Chan, N.W.C., Kraatz, H.-B., 2015. Investigation of the utility of complementary electrochemical detection techniques to examine the in vitro affinity of bacterial flagellins for a Toll-Like Receptor 5 biosensor. Anal. Chem.. http://dx.doi.org/10.1021/ac5042439.
Smit, J., Kamio, Y., Nikaido, H., 1975. Outer membrane of Salmonella typhimurium: chemical analysis and freeze-fracture studies with lipopolysaccharide mutants. J. Bacteriol. 124, 942–958.
Stokes, D.L., Griffin, G.D., Vo-Dinh, T., 2001. Detection of E. coli using a microfluidics-based antibody biochip detection system. Fresenius J. Anal. Chem. 369, 295–301. http://dx.doi.org/10.1007/s002160000660.
Su, W., Kim, S.-E., Cho, M., Nam, J.-D., Choe, W.-S., Lee, Y., 2013. Selective detection of endotoxin using an impedance aptasensor with electrochemically deposited gold nanoparticles. Innate Immun. 19, 388–397. http://dx.doi.org/10.1177/1753425912465099.
Su, W., Lin, M., Lee, H., Cho, M., Choe, W.S., Lee, Y., 2012. Determination of endotoxin through an aptamer-based impedance biosensor. Biosens. Bioelectron. 32, 32–36. http://dx.doi.org/10.1016/j.bios.2011.11.009.
Vo-Dinh, T., Griffin, G., Stokes, D.L., Wintenberg, A., 2003. Multi-functional biochip for medical diagnostics and pathogen detection. Sens. Actuators B: Chem. 90, 104–111. http://dx.doi.org/10.1016/S0925-4005(03)00048-0.
Wang, D., Hu, W., Xiong, Y., Xu, Y., Ming, Li, C., 2015. Multifunctionalized reduced graphene oxide-doped polypyrrole/pyrrolepropylic acid nanocomposite impedimetric immunosensor to ultra-sensitively detect small molecular aflatoxin B1. Biosens. Bioelectron. 63, 185–189. http://dx.doi.org/10.1016/j.bios.2014.06.070.
Witt, D., Klajn, R., 2004. Applications, properties and synthesis of omega-functionalized n-alkanethiols and disulfides-the building blocks of self-assembled monolayers. Curr. Org. Chem. 8, 1–34. http://dx.doi.org/10.2174/1385272043369421.
Yang, L., Bashir, R., 2008. Electrical/electrochemical impedance for rapid detection of foodborne pathogenic bacteria. Biotechnol. Adv. 26, 135–150. http://dx.doi.org/10.1016/j.biotechadv.2007.10.003.
Yang, M., Yang, Y., Liu, Y., Shen, G., Yu, R., 2006. Platinum nanoparticles-doped sol-gel/carbon nanotubes composite electrochemical sensors and biosensors. Biosens. Bioelectron. 21, 1125–1131. http://dx.doi.org/10.1016/j.bios.2005.04.009.
Yang, Z., Jian, Z., Chen, X., Li, J., Qin, P., Zhao, J., Jiao, X., Hu, X., 2015. Electrochemical impedance immunosensor for sub-picogram level detection of bovine interferon gamma based on cylinder-shaped TiO2 nanorods. Biosens. Bioelectron. 63, 190–195. http://dx.doi.org/10.1016/j.bios.2014.07.032.
Yeo, T.Y., Choi, J.S., Lee, B.K., Kim, B.S., Yoon, H.I., Lee, H.Y., Cho, Y.W., 2011. Electrochemical endotoxin sensors based on TLR4/MD-2 complexes immobilized on gold electrodes. Biosens. Bioelectron. 28, 139–145. http://dx.doi.org/10.1016/j.bios.2011.07.010.